Supplemental material

Supplemental figures

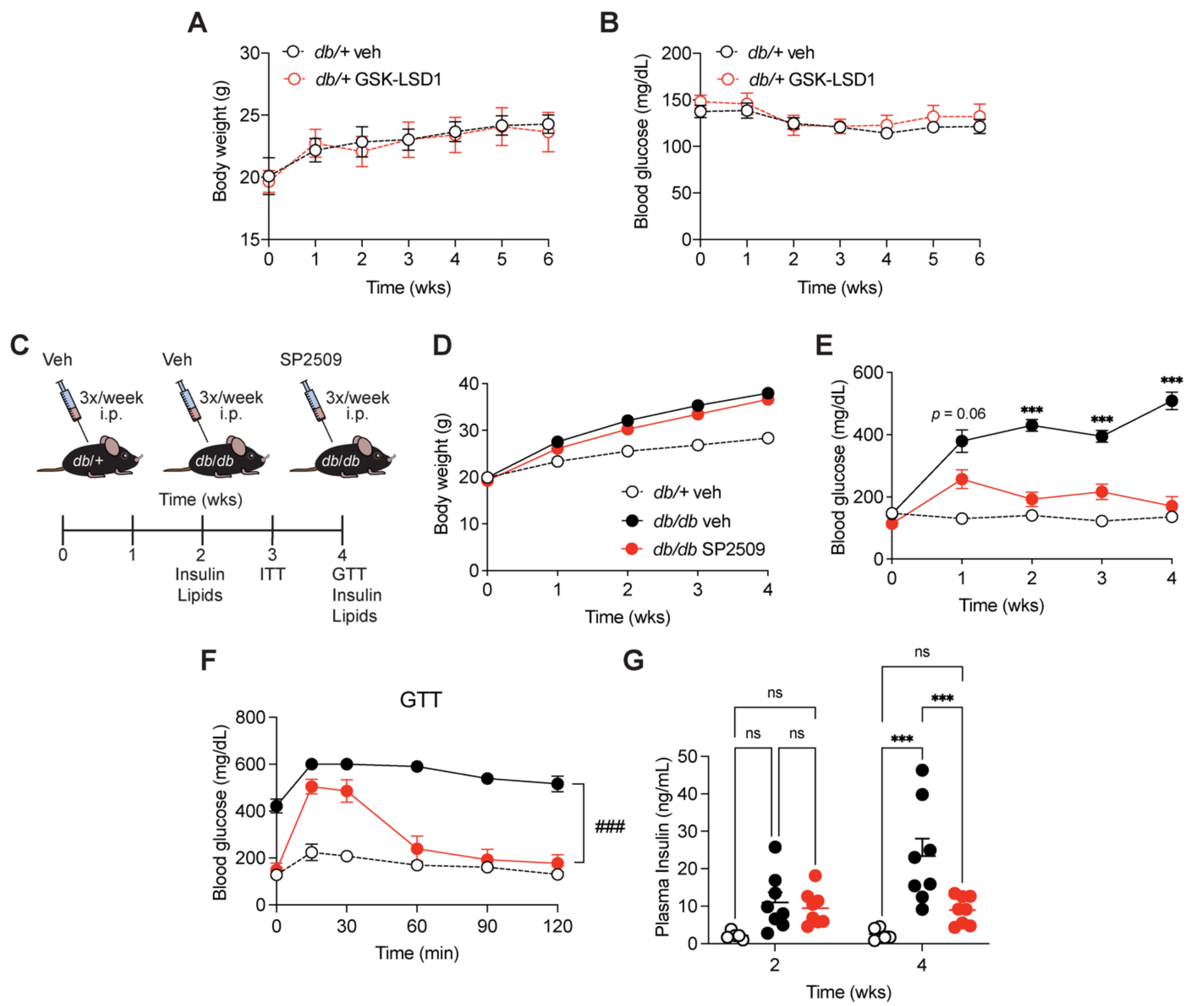

Figure S1. The structurally and mechanistically distinct LSD1 inhibitor SP2509 recapitulates effects of GSK-LSD1 on glucose homeostasis in *db/db* mice (**A**) Body weight and (**B**) blood glucose levels in 4-week-old male and female lean *db*/+ mice treated with GSK-LSD1 or vehicle (veh), respectively, for 6 weeks (n = 6 mice/group). (**C**-**G**) 4-week-old male and female *db*/*db* mice received SP2509 or vehicle (veh) thrice weekly via intraperitoneal injections for 4 weeks. As a control, lean *db*/+ mice were injected with veh. Metabolic measurements were conducted at the indicated time points. (**D**) Body weight and (**E**) blood glucose levels measured weekly (n = 5-8 mice/group). (**F**) Blood glucose levels at indicated time points after a glucose bolus via oral gavage (n = 5-8 mice/group). Glucose tolerance test, GTT. (**G**) Fasting plasma insulin levels after 2 and 4 weeks of SP2509 or veh treatment (n = 5-8 mice/group). Data are shown as mean ± SEM. Statistical differences were calculated using a two-way ANOVA with Tukey post hoc analysis. $^{***}p<0.001$, $^{###}p<0.001$, ns, not significant.

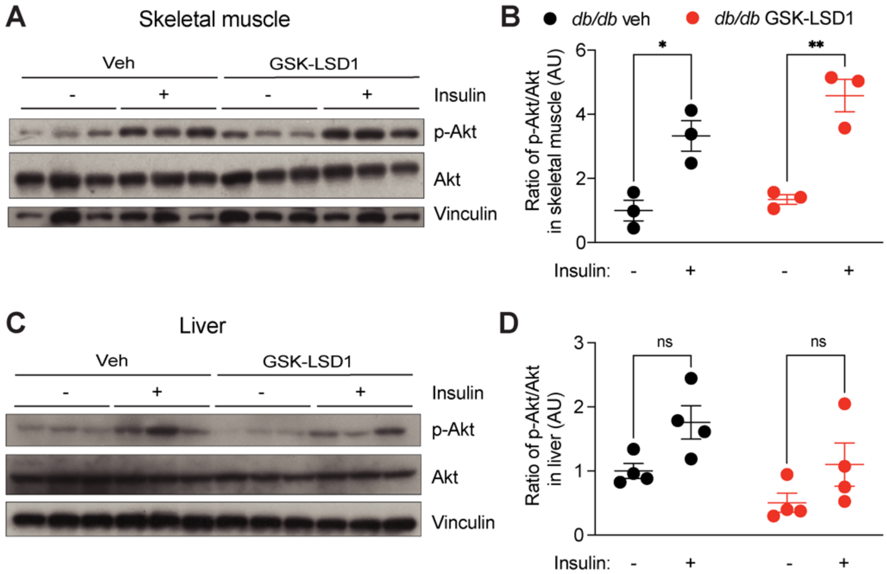

Figure S2. Impact of LSD1 inhibition on insulin sensitivity in peripheral tissues. (**A**-**D**) Immunoblot analysis of $pAkt^{Ser473}$, Akt, and vinculin in (**A**) skeletal muscle (n = 3 mice/group) and (**C**) liver (n = 4 mice/group). Quantification of $pAkt^{Ser473}$ to Akt ratio as fold change compared to veh-treated mice without insulin injection in skeletal muscle (**B**) and liver (**D**). Data are shown as mean ± SEM. Statistical differences were calculated using a two-way ANOVA with Tukey post hoc analysis. *p<0.05, **p<0.01. AU, arbitrary units, ns, not significant.

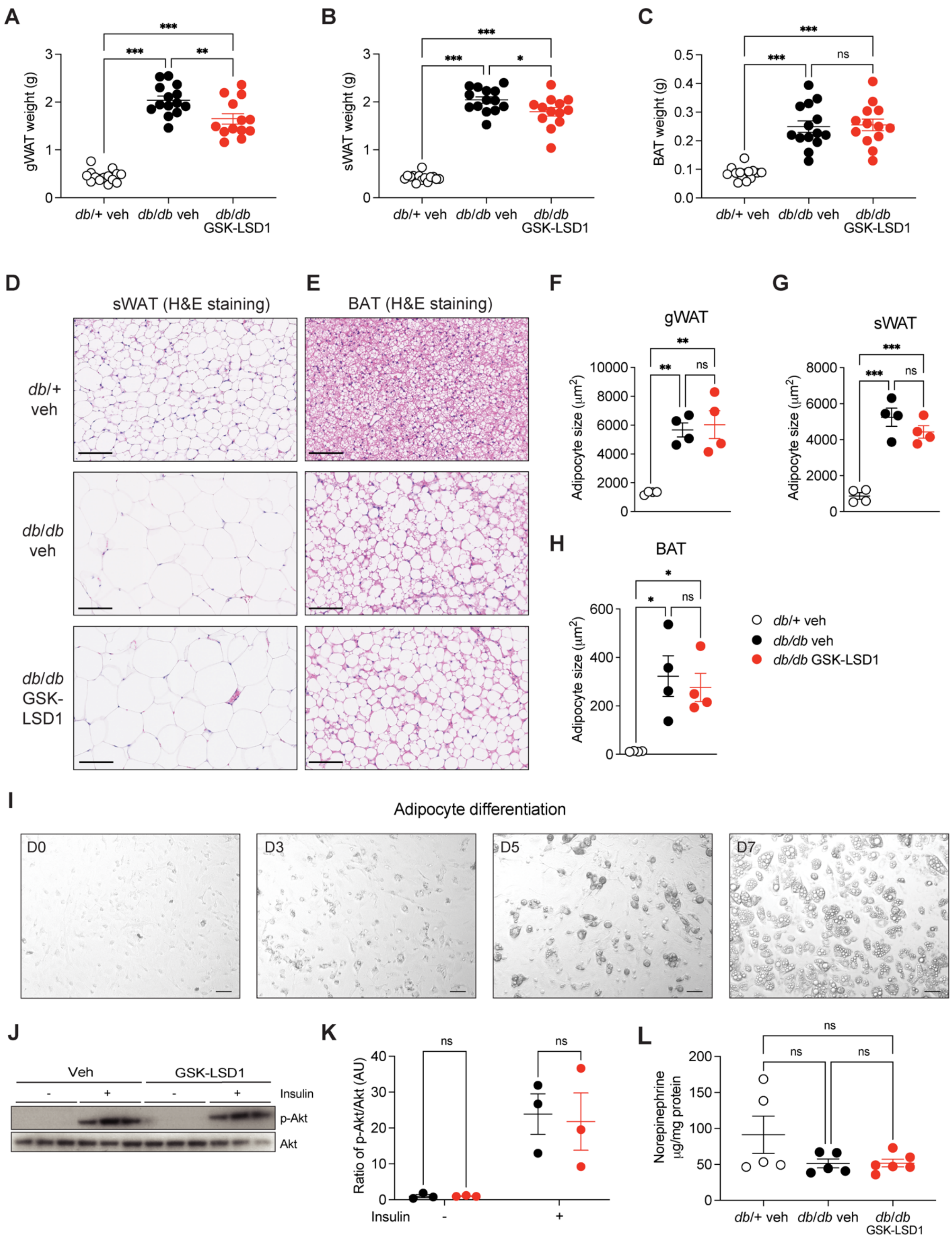

Figure S3. Impact of LSD1 inhibition on adipose tissue. (**A-H**) 4-week-old male and female *db/db* mice received daily intraperitoneal (i.p.) injections of GSK-LSD1 or vehicle (veh) for 6 weeks. As a control, lean *db/+* mice were injected with veh. Tissue weight of (**A**) gWAT, (**B**) sWAT, and (**C**) BAT (n = 13-14 mice/group). (**D**) Representative images of sWAT and (**E**) BAT sections stained with hematoxylin and eosin (H&E). Scale bars = 100 μm. (**F**) Adipocyte size quantified in gWAT, (**G**) sWAT, and (**H**) BAT (n = 4 mice/group). (**I**) Adipocytes were isolated from 5-week-old *db*/*db* mice. Representative images of adipocyte differentiation at day 0, 3, 5, and 7. Scale bars = 200 μm. (**J**) Immunoblot analysis of $pAkt^{Ser473}$ and Akt in differentiated adipocytes isolated from *db*/*db* mice after preincubation with GSK-LSD1 or veh and stimulation with insulin (n = 3 mice). (**K**) Quantification of $pAkt^{Ser473}$ to Akt ratio as fold change compared to veh-treated adipocytes. (**L**) WAT norepinephrine levels after 6 weeks of GSK-LSD1 or veh treatment of *db*/*db* mice or lean *db*/+ control mice (n = 5-6 mice/group). Data presented as mean ± SEM. A one-way ANOVA with Tukey post hoc analysis was performed to analyze statistical differences between three or more groups. *$p<0.05$, **$p<0.01$, ***$p<0.001$, ns, not significant.

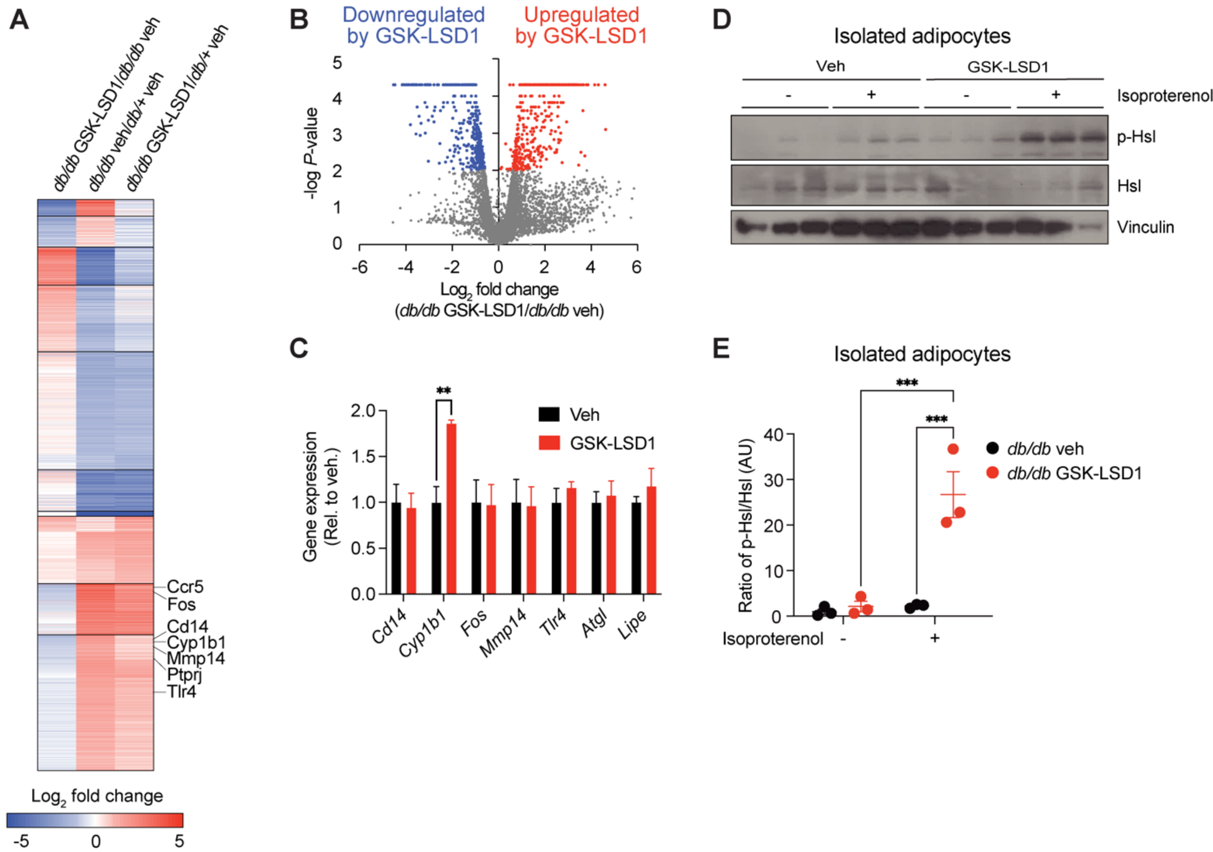

Figure S4. LSD1 inhibition in vivo reverses a subset of the effects of obesity on the gWAT transcriptome. (**A**) K-means clustering of $\log_2$ fold changes in mRNA levels in gWAT following 6 weeks of GSK-LSD1 treatment of male and female *db/db* mice, veh treatment of *db/db* mice, or veh treatment of *db/+* mice for the indicated comparisons. mRNAs differentially expressed in at least one pairwise comparison (*p*<0.01 by Cuffdiff) were used for clustering (n = 4 mice/group). (**B**) Volcano plot comparing mRNA levels in gWAT following GSK-LSD1 or veh treatment of *db/db* mice. Differentially expressed genes (*p*<0.01 by Cuffdiff) are indicated in red or blue. (**C**) Networks of genes upregulated (network nodes in red) or downregulated (network nodes in blue) by GSK-LSD1 compared to vehicle (*p*<0.01 by Cuffdiff) in gWAT from *db/db* mice following 6 weeks of treatment, shown as clustered functional categories (n = 4 mice/group). (**D**) qPCR of select inflammation genes downregulated by GSK-LSD1 from (A) as well as the lipolysis enzyme genes Atgl and Lipe (encoding Hsl) in differentiated adipocytes isolated from *db/db* mice after preincubation with GSK-LSD1 or veh. (**E**) Immunoblot analysis of $pHsl^{Ser660}$, Hsl, and vinculin in differentiated adipocytes isolated from *db/db* mice after preincubation with GSK-LSD1 or veh and stimulation with isoproterenol. (**F**) Quantification of $pHsl^{Ser660}$ to Hsl ratio as fold change compared to veh-treated adipocytes without isoproterenol. Data are shown as mean ± SEM. Statistical differences were calculated using Cuffdiff (B), multiple t-tests (C), or two-way ANOVA with Tukey post hoc analysis (E). ***p*<0.01, ****p*<0.001. AU, arbitrary units.

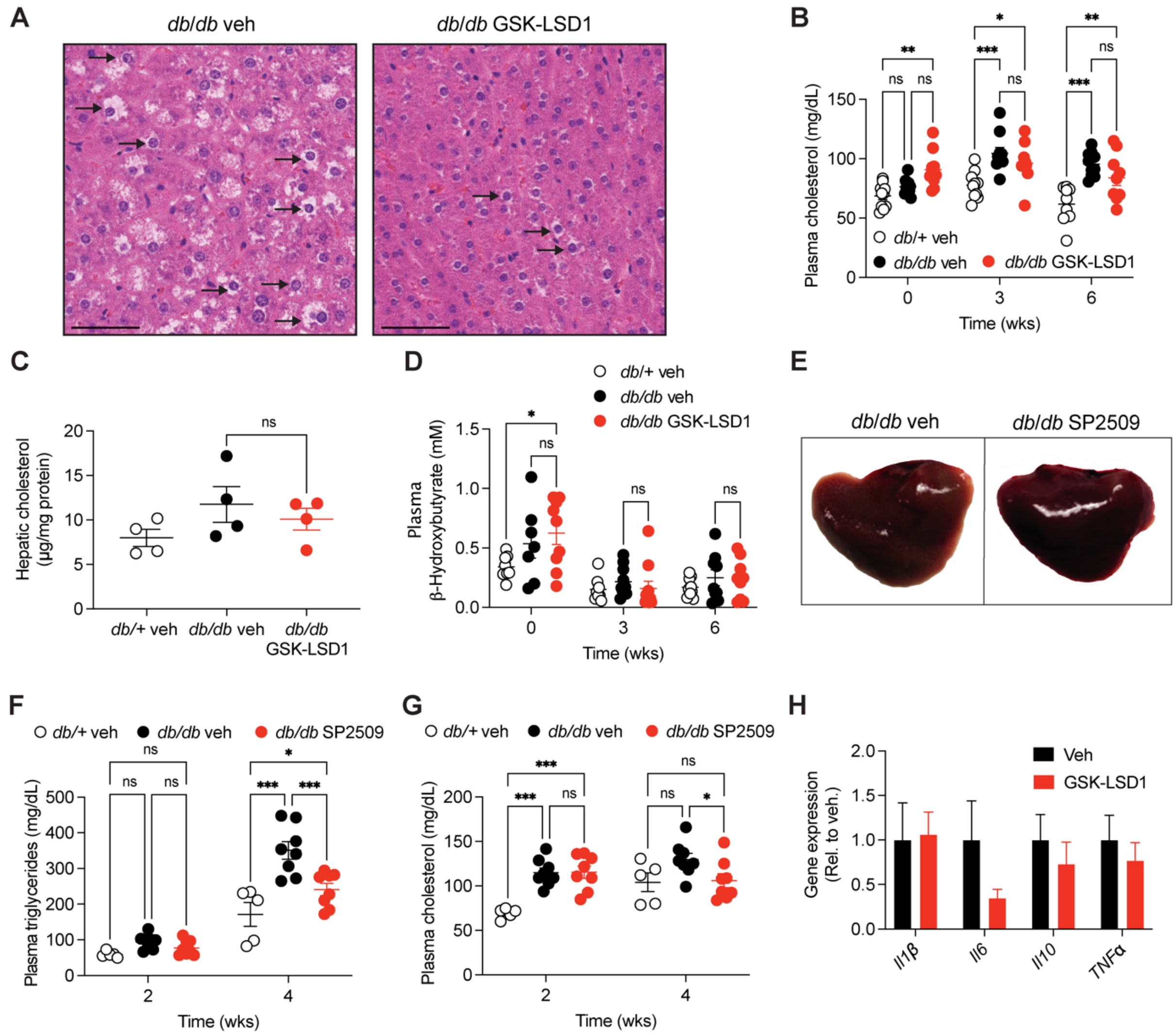

Figure S5. Plasma and hepatic metabolites in *db/db* mice. (**A**) 4-week-old male and female *db/db* mice received daily intraperitoneal injections of GSK-LSD1 or vehicle (veh) for 6 weeks. Representative images of H&E stains of livers. Examples of microvesicular steatosis are highlighted with an arrow. Scale bars = 50 µm. (**B**) Fasting plasma cholesterol levels at indicated time points (n = 9-10 mice/group). (**C**) Hepatic cholesterol levels (n = 4 mice/group). (**D**) Plasma β-hydroxybutyrate levels at indicated time points (n = 7-10 mice/group). (**E**-**G**) 4-week-old male and female *db/db* mice received SP2509 or vehicle (veh) thrice weekly via intraperitoneal injections for 4 weeks. As a control, lean *db*/+ mice were injected with veh. (**E**) Representative images of livers of *db/db* mice treated with SP2509 or vehicle (veh). (**F**) Fasting plasma triglyceride and (**G**) cholesterol levels at indicated time points (n = 5-8 mice/group). (**H**) qPCR analysis of inflammatory genes in liver. Transcript levels in GSK-LSD1-treated relative to veh-treated *db/db* mice (n = 6-8 mice/group). Data are shown as mean ± SEM. Statistical differences were calculated using multiple t-tests (H), a one-way ANOVA (C) or two-way ANOVA (B, D, F, G) with Tukey post hoc analysis. *$p<0.05$, **$p<0.01$, ***$p<0.001$, ns, not significant.

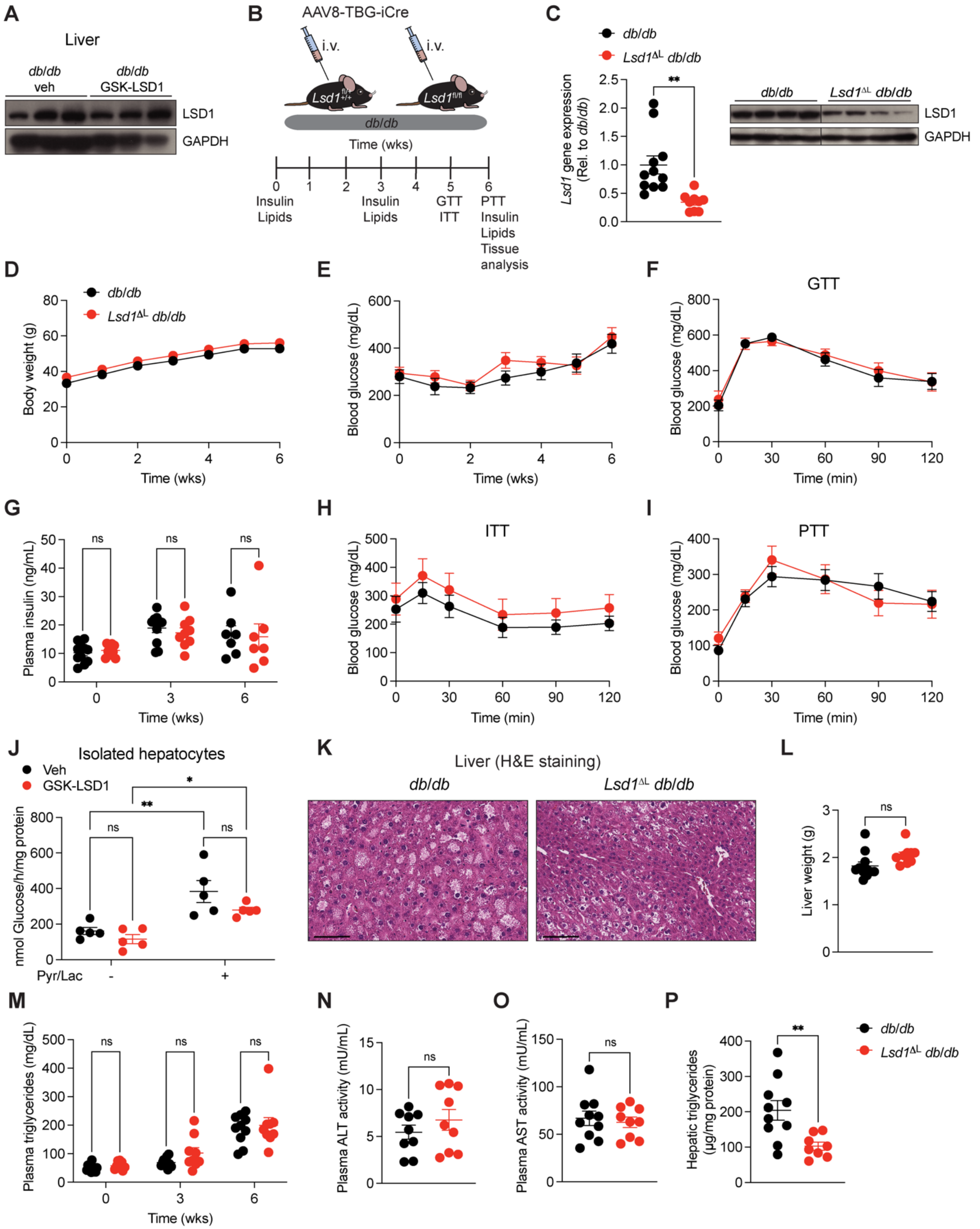

Figure S6: Hepatocyte-specific *Lsd1* deletion does not improve metabolic health in *db/db* mice. (**A**) Immunoblot analysis of LSD1 and GAPDH in the liver of GSK-LSD1- or vehicle (veh)-treated male and female *db/db* mice (n = 3 mice/group). (**B**) 5-week-old male and female *Lsd1*$^{fl/fl}$*db/db* or control (*Lsd1*$^{fl/+}$*db/db* and *Lsd1*$^{+/+}$*db/db*) mice were intravenously injected with

AAV8-TBG-iCre virus for hepatocyte-specific *Lsd1* deletion (hereafter referred to as $Lsd1^{\Delta L}db/db$ mice). (**C**) qPCR analysis of *Lsd1* in livers of $Lsd1^{\Delta L}db/db$ mice (left). Transcript levels relative to *db/db* control mice. (n = 9-11 mice/group). Immunoblot analysis of LSD1 and GAPDH in the liver of $Lsd1^{\Delta L}db/db$ and control mice (right). The lanes were run on the same gel but were noncontiguous (n = 4 mice/group). (**D**) Body weight and (**E**) blood glucose levels measured weekly (n = 9-11 mice/group). (**F**) Blood glucose levels at indicated time points after a glucose bolus via oral gavage (n = 9-11 mice/group). Glucose tolerance test, GTT. (**G**) Fasting plasma insulin levels at baseline and after 3 and 6 weeks of GSK-LSD1 or veh treatment (n = 9-11 mice/group for week 0 and 3, n = 7 mice/group for week 6). (**H**) Blood glucose levels at indicated time points after intraperitoneal insulin (2.0 U/kg body weight) injection (n = 9-11 mice/group). Insulin tolerance test, ITT. (**I**) Blood glucose levels at indicated time points after intraperitoneal pyruvate injection (n = 9-11 mice/group). Pyruvate tolerance test, PTT. (**J**) Glucose production in hepatocytes isolated from 5-week-old *db/db* mice after preincubation with GSK-LSD1 or veh overnight. Glucose release into the medium was measured after 2 hours of pyruvate and lactate stimulation (n = 5 mice). (**K**) Representative images of liver sections stained with hematoxylin and eosin (H&E). Scale bars = 100 µm (n = 5-7 mice/group). (**L**) Liver weight (n = 9-11 mice/group). (**M**) Fasting plasma triglyceride levels at indicated time points. (**N**) Plasma ALT and (**O**) AST activity (n = 9-11 mice/group). (**P**) Hepatic triglyceride levels (n = 8-10 mice/group). Data are shown as mean ± SEM. Statistical differences were calculated using an unpaired Student's t-test (L, O-P) or two-way ANOVA (D-J, M) with Tukey post hoc analysis. *p<0.05, **p<0.01, ***p<0.001, ns, not significant.

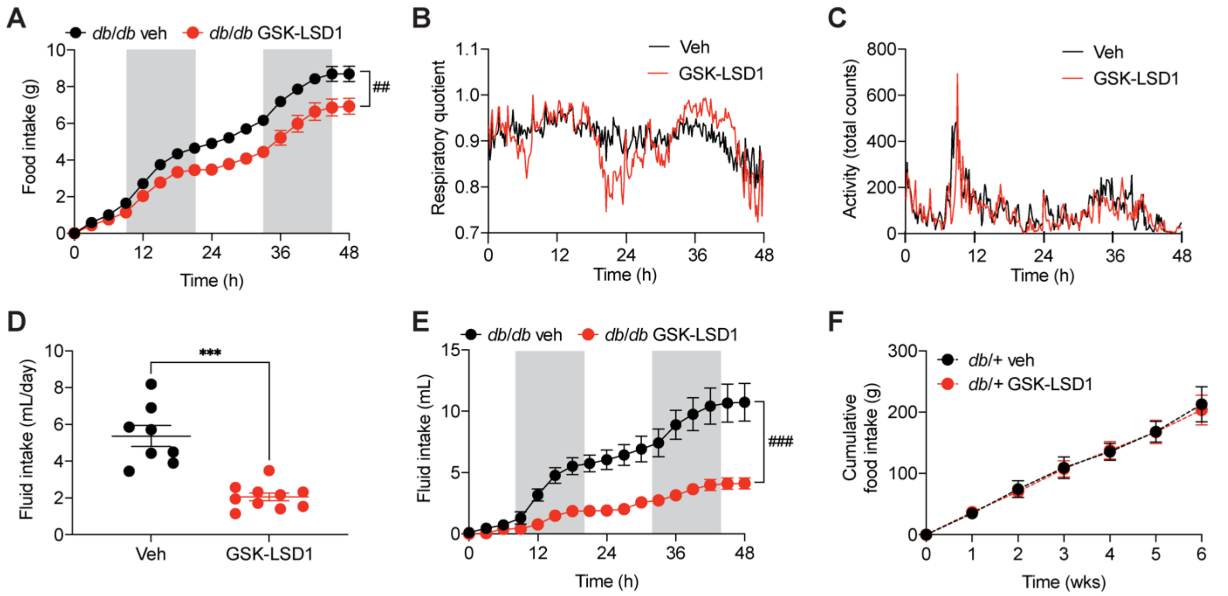

Figure S7. LSD1 inhibition does not alter energy expenditure in *db/db* mice. (**A**) Male and female m~~M~~ice were injected daily with GSK-LSD1 or vehicle (veh) for 5 weeks and then placed into metabolic cages. Using the Comprehensive Laboratory Monitoring System (CLAMS), food intake was monitored and is shown as additive food intake over 48 hours (n = 4-5 mice/group). (**B**) Respiratory quotient over the course of 48 hours (n = 4-5 mice/group). (**C**) Spontaneous motor activity along the X-, Y-, and Z- axis with IR photocells (n = 4-5 mice/group). (**D**) Daily water consumption (n = 4-5 mice/group/day) and (**E**) Cumulative water consumption (n = 4-5 mice/group). (**F**) Cumulative food intake in lean *db*/+ mice treated with GSK-LSD1 or veh for 6 weeks (n = 3 cages/group, total n = 7-9 mice/group). Data presented as mean ± SEM. Statistical differences were calculated using an unpaired Student's t-test (C) or two-way ANOVA (A, B, D-F) with Tukey post hoc analysis. *p<0.05, **p<0.01, ***p<0.001.

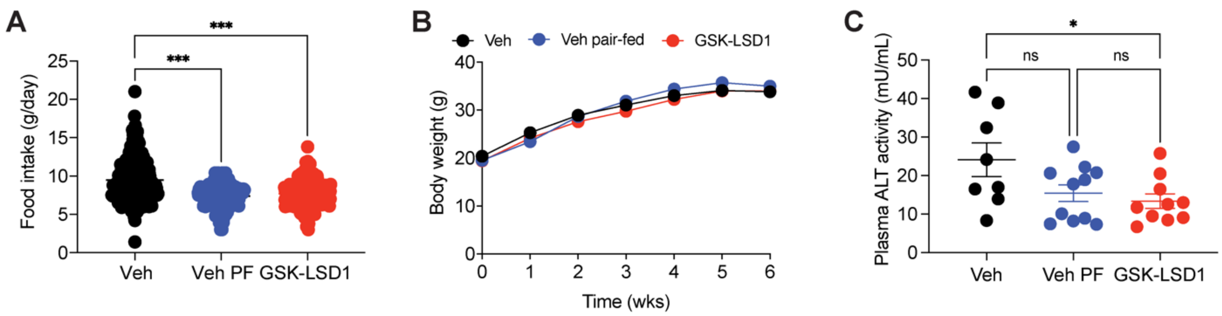

Figure S8. Metabolic parameters of pair-feeding study in *db/db* mice. (**A**) 4-week-old male and female *db/db* mice were injected daily with vehicle (veh) or GSK-LSD1 for 6 weeks and fed a normal chow diet ad libitum. A third group of mice received veh and was pair-fed to GSK-LSD1-treated mice. Food intake was measured daily (n = 8-11 mice/group/day). (**B**) Body weight measured weekly (n = 8-11 mice/group). (**C**) Plasma ALT activity (n = 8-11 mice/group). Data presented as mean ± SEM. Statistical differences were calculated using a one-way ANOVA (A, D) or two-way ANOVA (B, C) with Tukey post hoc analysis. *p<0.05, **p<0.01, ***p<0.001, ns, not significant.

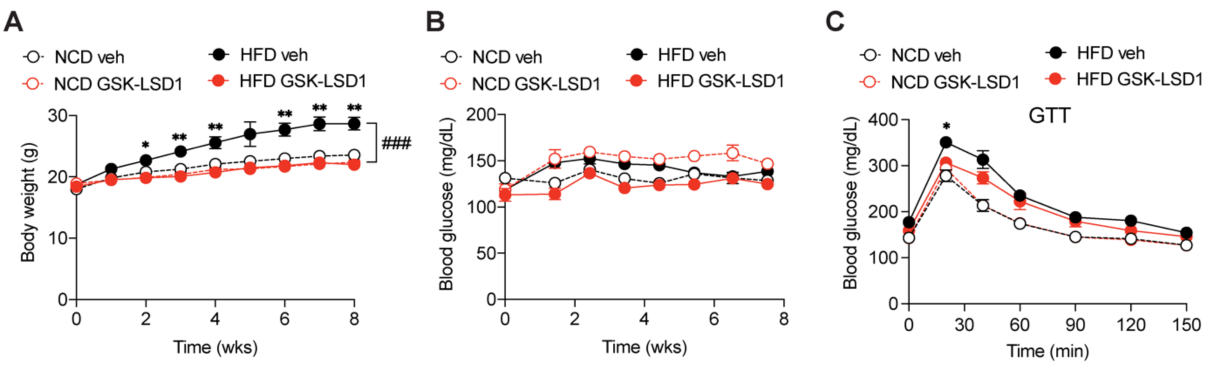

Figure S9. LSD1 inhibition prevents weight gain in high fat diet-fed mice. (**A**) 10-week-old male C57BL/6J *wild type* (*WT*) mice were fed a high fat diet (HFD) or normal chow diet (NCD) for 8 weeks and injected daily with GSK-LSD1 or vehicle (veh). (**B**) Body weight and (**C**) blood glucose levels measured weekly (n = 8 mice/group). Asterisks indicate statistical differences between HFD GSK-LSD1- and HFD veh-treated mice. (**C**) Blood glucose levels after 7 weeks of treatment at indicated time points after a glucose bolus via oral gavage (n = 8 mice/group). Glucose tolerance test, GTT. Asterisk indicates statistical difference between HFD GSK-LSD1 and HFD veh mice. Data presented as mean ± SEM. A two-way ANOVA with Tukey post hoc analysis was performed to determine statistical differences. *p<0.05, **p<0.01, $^{###}p$<0.001.

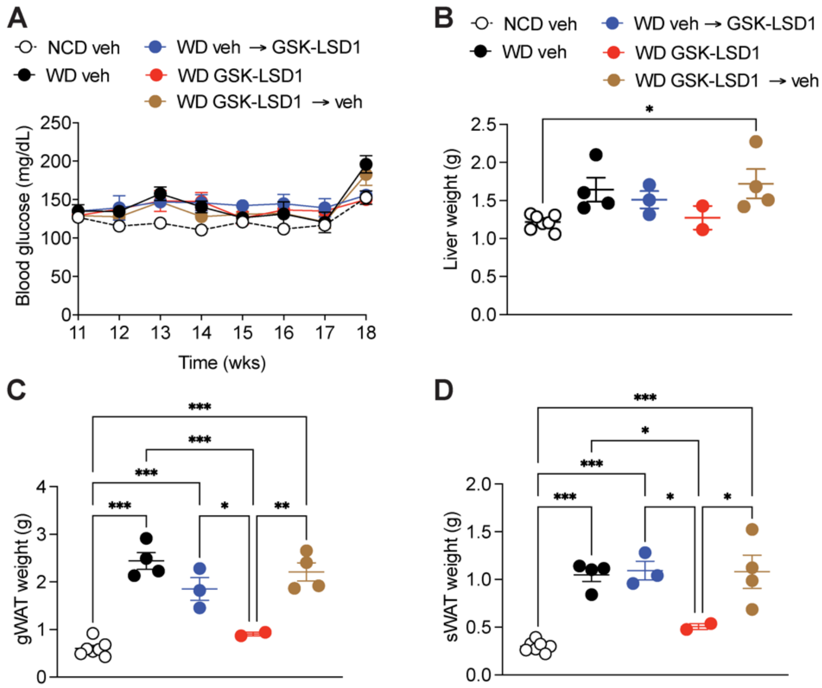

Figure S10. The effect of GSK-LSD1 on body weight in Western diet-fed mice is reversible. (**A**) 10-week-old male C57BL/6J mice fed a Western diet (WD) were injected daily with GSK-LSD1 or vehicle (veh) for 11 weeks. As a control, a group of mice received veh and was kept on a normal chow diet (NCD). After 11 weeks of veh administration, the veh group was split into one group continuing veh administration (black), whereas the other half began to receive GSK-LSD1 daily for another 7 weeks (blue). Likewise, the GSK-LSD1 group was split into one group continuing GSK-LSD1 administration after 11 weeks (red), whereas the other half began to receive veh daily for another 7 weeks (brown). Blood glucose levels were measured weekly (NCD veh: n = 7 mice, WD groups: n = 4 mice). (**B-D**) Tissue weights for (**B**) liver, (**C**) gWAT, and (**D**) sWAT (n = 2-7 mice/group). Data are shown as mean ± SEM. Statistical differences were calculated using a two-way ANOVA (A-D) with Tukey post hoc analysis. **p*<0.05, ***p*<0.01, ****p*<0.001.

Supplemental Table S1. List of quantitative PCR primers.

Gene	Forward Primer	Reverse Primer
Acc1	5’-CTTCCTGACAAACGAGTCTGG-3’	5’-CTGCCGAAACATCTCTGGGA-3’
Atgl	5’-AACACCAGCATCCAGTTCAA-3’	5’-GGTTCAGTAGGCCATTCCTC-3’
Ccl2	5’-CTCAGCCAGATGCAGTTAACG-3’	5’-AAACTACAGCTTCTTTGGGACAC-3’
Cd14	5’-GCCTTTCTCGGAGCCTATCT-3’	5’-TGGCTTCGGATCTGAGAAGT-3’
Cd36	5’-GAATTAGAACCGGGCCACGTA-3’	5’-CAGCCAGGACTGCACCAATA-3’
Cyp1b1	5’-TCCTCTCTGCCGAAAAGAAA-3’	5’-ACAACCTGGTCCAACTCAGC-3’
Elovl6	5’-GAAAAGCAGTTCAACGAGAACG-3’	5’-AGATGCCGACCACCAAAGATA-3’
Fabp1	5’-TGTGGTCAGCTGTGGAAAGG-3’	5’-CGGGCAGACCTATTGCCTTC-3’
Fasn	5’-GGAGGTGGTGATAGCCGGTAT-3’	5’-TGGGTAATCCATAGAGCCCAG-3’
Fos	5’-CGGGTTTCAACGCCGACTA-3’	5’-TTGGCACTAGAGACGGACAGA-3’

Il1β	5’-GAAATGCCACCTTTTGACAGTG-3’	5’-TGGATGCTCTCATCAGGACAG-3’
Il6	5’-TAGTCCTTCCTACCCCAATTTCC-3’	5’-TTGGTCCTTAGCCACTCCTTC-3’
Il10	5’-GCTCTTACTGACTGGCATGAG-3-	5’-CGCAGCTCTAGGAGCATGTG-3’
Lipe	5’-TGGTTCAACTGGAGAGCGGAT-3’	5’-TGATGCAGAGATTCCCACCTG-3’
Lsd1	5’-GCGCCATGGTCTTATCAACT-3’	5’-GCAACTCGTCCACCTACTCG-3’
Mmp14	5’-AAAGGCGCCCCAAGAGAG-3’	5’-GTCCCCTGGAGGTAGGTAGC-3’
Pklr	5’-GCCAGCAGGATACCTGAGAC-3’	5’-CATCCCTGCCTTGATCATCT-3’
Pparα	5’-AACATCGAGTGTCGAATATGTGG-3’	5’-AGCCGAATAGTTCGCCGAAAG-3’
Pparγ	5’-TCGCTGATGCACTGCCTATG-3’	5’-GAGAGGTCCACAGAGCTGATT-3’
Scd1	5’-TTCTTGCGATACACTCTGGTGC-3’	5’-CGGGATTGAATGTTCTTGTCGT-3’

Tbp	5’-GAAGCTGCGGTACAATTCCAG-3’	5’-CCCCTTGTACCCTTCACCAAT-3’
Tlr4	5’-GCTCCTGGCTAGGACTCTGA-3’	5’-AGAGGTGGTGTAAGCCATGC-3’
Tnfα	5’-CCTGTAGCCCACGTCGTAG-3’	5’-GGGAGTAGACAAGGTACAACCC-3’